EJN European Journal of Neuroscience

FENS Federation of European Neuroscience Societies

European Journal of Neuroscience, pp. 1–13, 2017 doi:10.1111/ejn.13551

Positive effects of neurofeedback on autism symptoms correlate with brain activation during imitation and observation

Michael Datko,[1,2,3] Jaime A. Pineda[1,3] and Ralph-Axel Müller[2]
[1]Department of Cognitive Science, UC San Diego, La Jolla, CA 92037, USA
[2]Brain Development Imaging Laboratory, Psychology, San Diego State University, San Diego, CA, USA
[3]Neurosciences, UC San Diego, La Jolla, CA, USA

Keywords: functional magnetic resonance imaging (fMRI), mirror neuron system, Mu-rhythm, plasticity, sociocommunication

Edited by Mark Wallace
Received 15 December 2016, revised 15 February 2017, accepted 22 February 2017

Abstract

Autism has been characterized by atypical task-related brain activation and functional connections, coinciding with deficits in sociocommunicative abilities. However, evidence of the brain's experience-dependent plasticity suggests that abnormal activity patterns may be reversed with treatment. In particular, neurofeedback training (NFT), an intervention based on operant conditioning resulting in self-regulation of brain electrical oscillations, has shown increasing promise in addressing abnormalities in brain function and behavior. We examined the effects of $\geq$ 20 h of sensorimotor mu-rhythm-based NFT in children with high-functioning autism spectrum disorders (ASD) and a matched control group of typically developing children (ages 8–17). During a functional magnetic resonance imaging (fMRI) imitation and observation task, the ASD group showed increased activation in regions of the human mirror neuron system following the NFT, as part of a significant interaction between group (ASD vs. controls) and training (pre- vs. post-training). These changes were positively correlated with behavioral improvements in the ASD participants, indicating that mu-rhythm NFT may be beneficial to individuals with ASD.

Introduction

Numerous findings support the hypothesis that social deficits in autism spectrum disorder (ASD) result from abnormal function in brain regions and networks associated with social cognition and action perception (Pelphrey & Carter, 2008; Misra, 2014). In particular, functional abnormalities have been observed in brain regions constituting the human mirror neuron system (hMNS) (Ramachandran & Oberman, 2006; Dapretto *et al.*, 2006; Hadjikhani *et al.*, 2006; Perkins *et al.*, 2010; although see Hamilton, 2013). The hMNS is a potential neurobiological substrate for many aspects of human social cognition, particularly those directly relevant to the behavioral and cognitive deficits observed in ASD (Williams *et al.*, 2001; Pineda, 2009), including the ability to comprehend actions, understand intentions, and learn through imitation. First described in single-unit recordings by Rizzolatti and colleagues in the macaque monkey (DiPelligrino *et al.*, 1992), mirror neurons are involved in both self-initiated action and the representation of action performed by others. Neurons in the monkey analog to the human pars opercularis of the inferior frontal gyrus (IFG) and in the inferior parietal lobule (IPL) show increased firing during execution and observation of the same action, representing a potential mechanism for mapping perceived biological motion onto the perceiver's sensorimotor systems (Rizzolatti & Craighero, 2004; Pineda, 2005). Indeed, a homologous network with similar functional properties has been described in humans using magnetoencephalography and functional magnetic resonance imaging (fMRI) (Hari *et al.*, 1998; Iacoboni, 1999; Buccino *et al.*, 2001).

Although some investigators have raised questions about the role of mirror neurons in human social behavior (Dinstein *et al.*, 2008; Hickok, 2009; Turella *et al.*, 2009), an increasing amount of work suggests that a dysfunction in the hMNS contributes to social deficits in ASD (Nishitani *et al.*, 2004; Oberman *et al.*, 2005; Théoret *et al.*, 2005; Dapretto *et al.*, 2006; Hadjikhani *et al.*, 2006; Bernier *et al.*, 2007; Perkins *et al.*, 2010; Oberman *et al.*, 2013). Individuals with ASD exhibit marked impairment in social skills, from joint attention to the theory of mind (Carpenter *et al.*, 1998; Baron-Cohen, 2009). More specifically, many studies show reduced activation in tasks involving social cognition and action imitation (Nishitani *et al.*, 2004; Oberman *et al.*, 2005; Dapretto *et al.*, 2006; Hadjikhani *et al.*, 2006; Williams *et al.*, 2006; Bernier *et al.*, 2007; Martineau *et al.*, 2008), some show increased activation (Martineau

Correspondence: Michael Datko, as above.
E-mails: mdatko@ucsd.edu; mikedatko@gmail.com

The associated peer review process communications can be found in the online version of this article.

et al., 2010), and in some instances selective abnormalities have been reported (Théoret *et al.*, 2005; Oberman *et al.*, 2008). A recent study showed functional and structural differences in connectivity between regions involved in action imitation in ASD (Fishman *et al.*, 2015). Notably, despite reduced activation, participants are still able to perform tasks related to social behaviors such as imitation – perhaps because of compensatory activation of other brain systems (Dapretto *et al.*, 2006) or normal hMNS function in specific social contexts (McIntosh *et al.*, 2006; Oberman *et al.*, 2008).

Studies using electroencephalography (EEG) have shown that putative electrophysiological biomarkers of hMNS activity show abnormalities in ASD (Oberman *et al.*, 2005, 2008; Bernier *et al.*, 2007). Accumulating evidence links the spectral dynamics of an EEG signal known as mu-rhythm to the hMNS (Pineda, 2005; Braadbaart *et al.*, 2013; Fox *et al.*, 2016). Particularly relevant is scalp-recorded EEG activity in the alpha mu (8–13 Hz) range that is most evident over the central scalp region overlying the sensorimotor cortices and is modulated by motor activity (Pfurtscheller & Neuper, 1994). More specifically, studies have indicated that low mu (8–10 Hz) is more related to nonspecific factors, such as attention, while high mu (10–12 Hz) reflects motor processing (Pfurtscheller *et al.*, 2000). Relative to baseline, mu-power is suppressed, not only during execution, but also during the observation and imagination of body movements (McFarland *et al.*, 2000; Pineda *et al.*, 2000; Muthukumaraswamy *et al.*, 2004; Pfurtscheller *et al.*, 2006). A multimodal study showed that suppression of mu-power is correlated with fMRI blood-oxygenation-level-dependent signal activations in areas associated with the hMNS (Arnstein *et al.*, 2011). In ASD, mu-rhythm suppression is absent during observation of body movements, supporting the role of an altered hMNS in the disorder (Oberman *et al.*, 2005; Oberman & Ramachandran, 2007). But, evidence suggests that the system is not beyond repair, because mu-suppression is intact when the people being imitated or observed are familiar to the ASD participant (Oberman *et al.*, 2008).

These findings motivate the use of neurofeedback training (NFT) in the context of treatment for ASD (Pineda *et al.*, 2012). This intervention has shown promise in research and clinical applications including lowering seizure incidence in epilepsy (Sterman, 1996; Walker, 2008), affecting corticomotor response to transcranial magnetic stimulation (Ros *et al.*, 2010) and brain activation during a Stroop task in unmedicated children with ADHD (Lévesque *et al.*, 2006). The NFT also requires less time to be efficacious compared with other behavioral interventions and produces fewer side-effects than pharmacotherapies (Fuchs *et al.*, 2003; Fox *et al.*, 2005). In terms of outcomes, a variety of studies demonstrate that the NFT produces positive behavioral and electrophysiological changes in children with ASD (Coben *et al.*, 2014; Pineda *et al.*, 2008, 2014; should add another researcher). Specifically, improvements in sociability and attention occur, as well as normalization of action-observation-related mu-rhythm suppression that is normally absent (Pineda *et al.*, 2008, 2014). Because mu-suppression is a putative index of hMNS activity, NFT targeting the mu-rhythm may be able to produce neuroplastic changes in this network. Because this system is thought to be critical for social behaviors, and functions abnormally in autism, mu-NFT could thus be beneficial in attenuating the social deficits in ASD. These observations led Coben *et al.* (2010) to argue that while further research is necessary, current studies support a Level 2 determination of 'possibly efficacious' for the application of neurofeedback in autism.

In the present study, we examined the effects of approximately ≥ 20 h of mu-NFT in a group of 17 high-functioning ASD children and a matched comparison group of 11 typically developing (TD) children, ages 8–17 years. We tested the prediction that NFT would produce changes in functional brain activation during an object-directed imitation task. More specifically, we predicted that before NFT, brain activation in the hMNS regions would be significantly lower in the ASD (compared with the TD) group, while following the NFT group differences in hMNS would be reduced. We also predicted that NFT-related changes in imitation-related brain circuits would be more pronounced in the ASD group, where imitation behavior, hMNS activation, and mu-rhythm dynamics are compromised, compared with the TD group. Finally, we predicted that the severity of social symptoms in autism would be reduced following training, and that this reduction would correlate with changes in fMRI activation.

Methods

Participants

Seventeen high-functioning ASD (mean age = 12.51 ± 0.76; 13 male; IQ > 80) and 11 TD participants (mean age = 10.64 ± 0.75; seven male) were recruited for the study. Participants were recruited from San Diego and Los Angeles Counties via local support groups for children with ASD and other disabilities, from local schools and recruitment posters, and via Valerie's List, a San Diego internet-based autism support group. Participants and parents gave informed assent and consent, respectively, in accordance with the Helsinki Declaration. The University of California, San Diego's Institutional Review Board approved the study. All but three participants in the ASD group had their diagnoses verified by a clinician immediately before our study using the Autism Diagnostic Observation Schedule (ADOS) (Lord *et al.*, 2000) and Autism Diagnostic Interview (ADI) (Rutter *et al.*, 2003), and all but one met the criteria of high-functioning autism with an IQ greater than 80 based on the Wechsler Abbreviated Scale of Intelligence (WASI) (Wechsler, 1999). For the three participants whose diagnoses were not based on ADOS or ADI, we used their psychoeducational evaluations, which are a component of the triennial evaluation required of all special education students in the San Diego school district. One participant received intelligence testing using the Kauffman Assessment Battery for Children (Cahan & Noyman, 2001) instead of the WASI.

Seven of the ASD participants and four of the TD participants were excluded from the final statistical analyses because of excessive head motion during one or both fMRI sessions (four ASD, one TD), inability to complete the post-training fMRI scan (two ASD), structural brain abnormality preventing proper registration in standard space (one ASD), or inability to complete the NFT (three TD). Following these exclusions, groups were matched for age and WASI IQ. Demographic and diagnostic information is summarized in Table 1.

Neurofeedback training

The training process involved EEG recordings from the C4 electrode over right sensorimotor cortex and extracting power in the mu-frequency band (8–13 Hz), which was in turn used to control a video game or movie. Both the game and movie activities required keeping mu-power above a threshold, which was determined before each session based on the participant's 1-min baseline amplitude at the start of the session. Training also included inhibiting amplitude in other specified EEG frequencies (theta: 4–8 Hz and beta: 13–30 Hz) and keeping them below a pre-defined amplitude threshold as per standard protocols (Othmer, 2012). During training, participants saw

TABLE 1. Participant demographic, diagnostic, and behavioral information. (A) Only subjects with usable fMRI data. (B) Same as (A) but for all recruited subjects, including those that did not complete post-NFT fMRI scanning sessions

	ASD (n = 10, three female, one left-handed) Mean (SEM) Range	TD (n = 7, two female, one left-handed) Mean (SEM) Range	P
(A) Demographic and diagnostic information for participants with usable fMRI data			
Age	13.3 (0.98) 9.26–18.3	11.3 (0.92) 8.64–16.7	0.20
WASI: Full-scale IQ	101.1 (7.65) 56–134	115.6 (2.95) 104–130	0.16
WASI: verbal IQ	99.1 (7.06) 55–130	111.6 (2.91) 97–127	0.19
WASI: non-verbal IQ	98.6 (7.93) 62–137	113.0 (3.81) 103–137	0.18
SRS total (pre-NFT)	75.6 (3.82) 58–90	38.6 (1.20) 35–46	5.26E-07
SRS total (post-NFT)	68.7 (3.36) 56–90	38.8 (0.76) 35–42	1.49E-06
SRS post- vs. pre-NFT	$P = 095^{\dagger}$	$P = 0.692$	N/A
ADOS: Com + Soc	11.55 (1.70) 3–22	N/A	N/A
ADI-R: Soc	15.33 (2.44) 6–28	N/A	N/A
ADI-R: Com	14.11 (2.18) 4–23	N/A	N/A
ATEC total (pre-NFT)	38.7 (4.40) 15–65	N/A	N/A
ATEC total (post-NFT)	27.2 (3.95) 7–51	N/A	N/A
ATEC post- vs. pre-NFT (P<)	$P = 0.034^{*\dagger}$	N/A	N/A
	ASD (n = 17, four female, two LH) Mean (SEM) Range	TD (n = 11, four female, one LH) Mean (SEM) Range	P
(B) Demographic and diagnostic information including participants without usable fMRI data			
Age	12.5 (0.76) 9.07–18.3	10.64 (0.75) 8.39–16.69	0.109
SRS total (pre-NFT)	79.5 (2.70) 58–90	38.6 (1.1) 35–46	5.26E-07
SRS total (post-NFT)	70.6 (2.65) 56–90	38.8 (0.74) 35–42	1.49E-06
SRS post- vs. pre-NFT	$P = 0.013^{*\dagger}$	$P = 0.87$	N/A
ATEC total (pre-NFT)	42.06 (3.43) 15–67	N/A	N/A
ATEC total (post-NFT)	30.8 (3.67) 7–54	N/A	N/A
ATEC post- vs. pre-NFT (P<)	$P = 0.016^{*\dagger}$	N/A	N/A

*Significance at $P < 0.05$.
†That a one-tailed hypothesis-driven t-test was used.

a display of three threshold bars alongside the game/movie window. One corresponded to the rewarded mu-frequency and the other two corresponded to the inhibited frequencies. Rewards (e.g., a car moving faster around a race track on the screen, or an increase in the size of the video playback while viewing a movie) were given based on satisfying two conditions: (i) power in the specified frequency (8–13 Hz mu-band) exceeded each participant's individually set threshold, and (ii) power from the theta (related to blinks) and beta (related to muscle movement) activity was below threshold. Theta and beta inhibition feedback was included in the design for two reasons. First, it ensured that individuals could not advance in the game or expand the DVD viewing window by producing movement-induced power increases across the entire EEG spectrum. Second, it allowed for distinguishing between improvement effects as a function of EEG modulation as opposed to modulation of autonomic nervous system and muscle activity. because of scheduling issues, not all participants reached the target of 30 h of training on a regimen of two 45-min training sessions per week for 20 weeks. Actual training varied individually between 20 and 30 h, as detailed in Table 2A.

To demonstrate that learning occurred as a result of the NFT, and that subjects improved their ability to modulate mu on demand during the sessions, we measured the relationship between two values in each session: mu-amplitude during a baseline period of one minute before the beginning of each session, and average mu-amplitude over the course of the session itself. Increased baseline or session mu-power by themselves, over the course of all sessions would not necessarily indicate that subjects were improving in their ability to increase mu-volitionally when asked to do so during the session. Therefore, for each session, we calculated a log ratio between these two values as: $\mathrm{Log}_{10}\ (\mathrm{Mu}_{\mathrm{Session}}/\mathrm{Mu}_{\mathrm{Baseline}})$.

We also calculated this ratio for two subdivisions of the mu-band (8–10 and 10–12 Hz) to separate nonspecific from specific effects. Subjects' improved ability to volitionally increase amplitude over the threshold over the course of training sessions was measured by calculating the Pearson correlation between the number of sessions completed by each subject and the log ratio of session power to baseline power. Those values were normalized by performing a Fisher transformation to ensure a more normal distribution for further statistics.

Behavioral assessments

Two pen-and-paper questionnaires, the Autism Treatment Evaluation Checklist (ATEC) (Magiati *et al.*, 2011) and the Social Responsiveness Scale (SRS) (Constantino *et al.*, 2003), were given to one of the parents of each participant before and after training. Scores are summarized in Table 1A (see Supporting information for details).

Imitation task

All participants performed an imitation task during fMRI. See Supporting information for detailed scanning parameters, and methods for preprocessing and analysis of fMRI data. We tested the prediction that NFT would produce changes in functional brain activation during an object-directed imitation task based on a previous study that required

TABLE 2. Group behavioral data. (A) Training and sessions completed. (B) Imitation task accuracy and reaction time. (C) Head motion and timepoint censoring

(A) Training and sessions completed			
Total hours training	26.4 (1.72) 14.75–33.75	17.2 (1.69) 9–21.5	0.003
Total training sessions	36.4 (3.15) 20–50	18.4 (1.77) 10–24	0.0006
Days between first to last training session	211.6 (26.7) 78–335	328.0 (51.8) 179–563	0.073
Training density (hours per month)	4.25 (0.39) 2.69–5.76	1.79 (0.26) 1.09–3.18	0.0004
	ASD (n = 10) Mean (SEM) range	TD (n = 7) Mean (SEM) range	P
(B) Imitation task accuracy and reaction time			
Pre-training % correct trials	83.8% (3.93) 64–97	86.6% (3.66) 63–97	0.32
Pre-training reaction time (correct trials)	1.153 s (0.019) 0.067–3.25	1.137 s (0.023) 0.07–2.89	0.58
Post-training % correct trials	86.0% (6.41) 47–100	87.5% (6.87) 40–100	0.45
Post-training reaction time (correct trials)	1.234 s (0.024) 0.126–2.91	1.103 s (0.021) 0.354–2.90	< 0.0001
Post- vs. pre-NFT % correct trials	P = 0.39	P = 0.46	
Post- vs. pre-NFT reaction time (correct trials)	P = 0.01	P = 0.28	
(C) Head motion and timepoint censoring			
Pre-training total motion RMSD (pre-censoring)	0.173 (0.034) 0.04–0.35	0.169 (0.034) 0.03–0.34	0.47
Pre-training percent censored	8.6% (4.0) 0–41	14.0% (4.2) 1–38	0.21
Pre-training total motion RMSD (post-censoring)	0.13 (0.02) 0.04–0.27	0.11 (0.018) 0.03–0.21	0.29
Post-training total motion RMSD (pre-censoring)	0.125 (0.026) 0.04–0.29	0.101 (0.014) 0.06–0.17	0.25
Post-training percent censored	1.4% (0.78) 0–8	0.85% (0.47) 0–4	0.31
Post-training total motion RMSD (post-censoring)	0.11 (0.021) 0.035–0.24	0.09 (0.01) 0.06–0.15	0.20
Post- vs. Pre-NFT RMSD (pre-censoring)	P < 0.14	P < 0.08	
Post- vs. Pre-NFT percent censored	P < 0.047	P < 0.01	
Post- vs. Pre-NFT RMSD (post-censoring)	P < 0.28	P < 0.18	

RMSD, root mean squared deviation.

participants to observe or imitate simple finger-lifting actions (Iacoboni, 1999). These conditions elicited activation in two areas associated with the hMNS: the IPL and superior temporal sulcus (STS). The task has also been used to demonstrate activation differences between ASD and TD groups in those two areas (Williams *et al.*, 2006). However, the study by Williams and colleagues did not show activation or significant group differences in IFG. This lack of activation is critical because IFG is considered a core component of the hMNS (Rizzolatti & Craighero, 2004) and is one of the potential sites of NFT-related plasticity. Therefore, for the present study, we used a modified version of this task by having participants observe a hand pressing buttons and imitate those actions on an identical button box (Fig. 1). This changed the task from requiring imitation and observation of meaningless movement to one based on object-directed movement. This type of action has been shown to elicit stronger activations in mirror areas, specifically in IFG (Muthukumaraswamy *et al.*, 2004), making our task more appropriate for a comprehensive study of differences in mirroring-related activation between ASD and TD participants.

Activation during the different conditions shown in Fig. 1 was combined into three contrasts: imitation, observation, and imitation + observation. For imitation, activations during Conditions 2 and 3 were subtracted from Condition 1. For observation, activations during Conditions 5 and 6 were subtracted from Condition 4. Finally, the imitation and observation contrasts were averaged together to create the imitation + observation contrast.

For each of the three contrasts, two separate whole-brain t-tests were performed to compare activation between ASD and TD groups: one for pre-NFT activation and another for post-NFT. Two additional whole-brain t-tests were performed for pre- vs. post-NFT activation within each group (i.e. ASD pre- vs. ASD post-training). All t-tests were family wise error rate (FWER) corrected for multiple comparisons at the cluster level to $P < 0.05$ (Forman *et al.*, 1995).

For each contrast, a whole-brain analysis of variance (ANOVA) was performed on the brain activation data, with group status (ASD, n = 10; TD, n = 7) and training status (pre-NFT or post-NFT) as the two main factors. The results passed an uncorrected voxelwise threshold of $P = 0.02$ and were then FWER-corrected for multiple comparisons at the cluster level to $P < 0.05$.

ANOVAS were then performed for each contrast to test for interactions between group (ASD and TD) and training status (pre-NFT and post-NFT) in two different sets of regions of interest (ROIs). One set of the ROIs was derived from a meta-analysis of 87 fMRI studies of imitation that identified fourteen consistently activated regions (Caspers *et al.*, 2010). Center coordinates for each ROI listed in that study were converted from MNI to Talairach space (Talairach & Tournoux, 1988) (Table 6), and spherical ROIs with a 7 mm radius were created around them. A second set of seven ROIs was created from the activation maps for the imitation + observation contrast in ASD and TD groups pooled together. Coordinates of each ROI's center of mass were used as the center coordinates (Table 6) for seven spherical ROIs with 7 mm radius.

Covariance of ASD symptom severity and brain activation

Finally, we investigated whether ASD symptom severity covaried with the changes in fMRI activation between post- vs. pre-NFT scans. Specifically, we performed separate whole-brain analysis of covariance (ANCOVA) tests comparing the pre-NFT to post-NFT activation in the ASD group, with ADOS (sociocommunicative subscale), ADI (social subscale), ATEC, and SRS scores as covariates. While the ADOS and ADI scores only had one score per participant, ATEC and SRS scores from before and after NFT were converted into a difference score for each participant (equal to the post-NFT score minus pre-NFT score for each measure) to facilitate their use as covariates. All results passed an uncorrected voxelwise threshold of $P = 0.02$ and remaining clusters were FWER-corrected for multiple comparisons to $P < 0.05$.

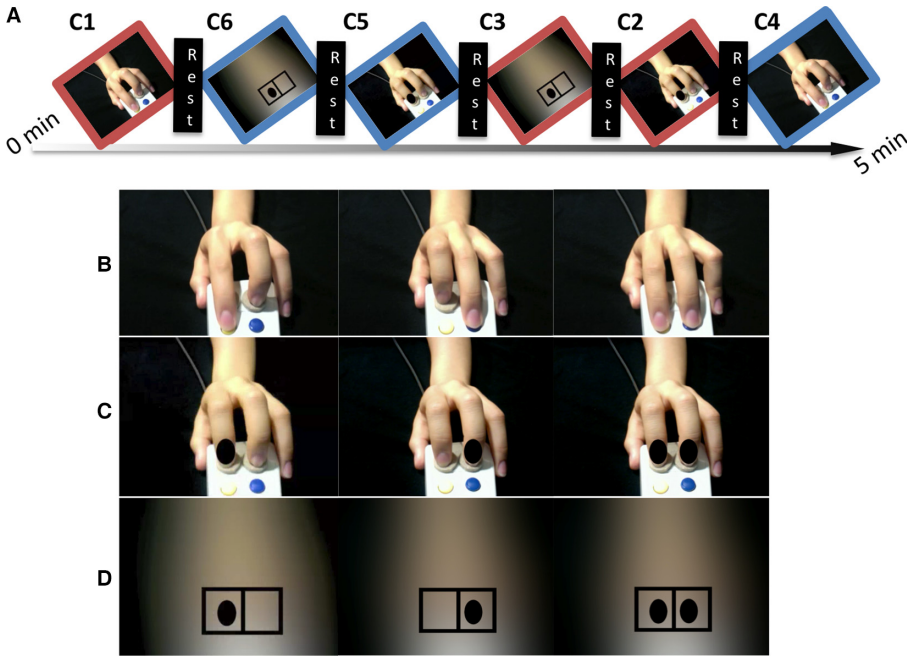

FIG. 1. (A) The task included three 5-min runs, each containing 27-s blocks of each of six conditions and five 20-s rest periods (with a fixation cross). (B) Instructions were to imitate finger movements shown in videos of a hand pressing one or both buttons on a button box. (C) Condition 2 controlled for visual movement: stimuli were still images, instead of movies, of the same hand and button box, with a black dot in front of either or both of the fingers as an indicator of which button to press. (D) Condition 3 controlled for spatial features: a blurred background with the same luminance as the hand picture was shown, with black dots within a rectangle as the indicators of which button the participant should press. Each block contained nine stimuli (three each for index, middle, and both fingers) shown in pseudo-random order for 2.5-s each, with 0.5-s inter-stimulus intervals. In Conditions 4–6 (blue borders), stimuli were identical to those in Conditions 1–3 (red borders), but participants were instead instructed to observe and pay attention without responding (Observation during video stimuli = Condition 4; observation of still images = Condition 5; observation of blurred still images = Condition 6).

Results

Behavioral

We computed the correlation between post-NFT minus pre-NFT imitation activation changes (with each of the four clusters of group × training interaction individually) and the session power correlations, and determined the *P*-value for that correlation. For each group individually, these correlations were not significant (example for cluster in right IPL: ASD $r = 0.52$, $P = 0.188$; TD $r = 0.36$, $P = 0.424$). Collapsing across both ASD and TD groups, there was a significant and positive correlation between fMRI task activation change in the cluster in right IPL (Cluster 1 on Table 5) and the ratio of mu/baseline session power across sessions ($r = 0.52$, $P = 0.049$). This effect was slightly stronger when specifically looking at low alpha instead (8–10 Hz, $r = 0.57$, $P = 0.028$), but not high alpha (10–12 Hz, $r = 0.28$, $P = 0.31$).

Groupwise accuracy and reaction time data for the imitation task are summarized in Table 2B. Correct trials were trials in which the participant accurately imitated and pressed the same button or buttons as presented on the screen. Accuracy on the imitation task did not differ significantly between groups either pre-NFT (ASD $M = 83.8\%$, TD $M = 86.6\%$, $P = 0.65$) or post-NFT (ASD $M = 86.0\%$, TD $M = 87.5\%$, $P = 0.89$), or within groups pre- vs. post-NFT (ASD $P = 0.77$, TD $P = 0.93$). Reaction time on correct trials did not differ between groups pre-NFT (ASD $M = 1.15$ s, TD $M = 1.15$ s, $P = 0.99$) or post-NFT (ASD $M = 1.28$ s, TD $M = 1.09$ s, $P = 0.43$), or within groups pre- vs. post-NFT (ASD $P = 0.54$, TD $P = 0.59$).

Group averages for root mean squared deviation of head motion during the task scans are summarized in Table 2C. There were no significant group differences in head motion either between groups or within groups before vs. after the training.

Pen-paper/parental assessment data

Between-group *t*-tests were performed on the data from each pen-paper and parental assessment collected. Group averages, as well as the results of these statistical tests are summarized in Table 1A (subset of subjects with usable fMRI data) and Table 1B (full sample of subjects who completed the NFT, with or without usable fMRI data). For the subset, groups did not significantly differ on age (ASD $M = 13.3$; TD $M = 11.3$, $P = 0.20$) or WASI scores for either the full-scale (ASD $M = 101.1$; TD $M = 115.6$, $P = 0.16$), verbal only (ASD $M = 99.1$; TD $M = 111.6$, $P = 0.19$), or non-verbal only WASI (ASD $M = 98.6$; TD $M = 113.0$, $P = 0.18$).

The ASD group showed significant improvements in the SRS for the full sample after NFT (pre-NFT $M = 79.5$; post-NFT $M = 70.6$; $P = 0.013$), but only approached significance for the subset (pre-NFT $M = 75.6$; post-NFT $M = 68.7$; $P = 0.095$). For the ATEC, the ASD group showed significant improvements for both the full sample (pre-NFT $M = 42.06$; post-NFT $M = 30.8$; $P = 0.016$) and the subset (pre-NFT $M = 38.7$; post-NFT $M = 27.2$; $P = 0.034$).

Activation for imitation and observation combined

Results reported here are for the combined imitation+observation contrast only. Results for the two separate imitation and observation contrasts are in Supporting information. Pre-NFT, the TD group showed clusters of activation in hMNS areas including left IPL, left superior parietal lobule, bilateral IFG, and bilateral STS. The ASD group showed clusters of activation in left STS and bilateral cuneus. On between-group tests, the ASD participants had significantly lower activation compared with the TD group in precuneus, cingulate cortex, bilateral inferior temporal cortex, left premotor cortex, and right IFG (Table 3, Fig. 2A).

TABLE 3. Pre-NFT BOLD activation for Imitation + Observation contrast

Group	Peak location	Hemi	*x*	*y*	*z*	Voxels	Volume (μL)	Peak *Z*-score
TD[†]	Mid Occ, pMTS, pSTS	R	−51	68	−5	279	837	4.56
	Mid Occ, pMTS, pSTS	L	48	61	−2	156	468	5.65
	Inferior parietal lobule (BA 40)	L	31	51	39	40	120	4.19
	Superior parietal lobule (BA 7)	L	31	58	53	35	105	3.51
	Inferior frontal gyrus (BA 45, 46)	R	−44	−24	19	34	102	4.79
	Precuneus	R	−17	75	39	28	84	4.77
	Inferior frontal gyrus (BA 44)	L	41	−4	25	25	75	3.79
	Precentral (BA 4,6)	R	−44	10	53	20	60	5.01
	Precentral (BA 4)	L	27	20	66	20	60	3.65
	Inferior parietal lobule (BA 40)	L	34	37	39	16	48	3.72
ASD	Lateral occipital	R	−54	64	−2	53	159	3.48
	Lateral occipital	L	51	68	5	44	132	4.41
	Superior temporal gyrus	R	−65	37	15	33	99	4.04
ASD > TD	Precuneus	R	−10	78	43	81	243	3.13
	Cingulate gyrus	L	10	−11	32	68	204	4.69
	Inferior temporal/lat. occipital	L	48	58	−16	61	183	2.73
	Posterior cingulate	R	−20	58	−2	35	105	4.78
	Cuneus/calcarine gyrus	L	10	75	8	33	99	4.03
	Fusiform gyrus	R	−54	58	−9	30	90	3.03
	Middle temporal (BA 21, 22)	R	−54	41	5	28	84	3.16
	Precentral gyrus (BA 4,6)	L	14	27	59	27	81	3.04
	Inferior frontal gyrus (BA 45, 13)	R	−44	−24	19	25	75	4.16

[†]Subcortical clusters not listed. All clusters $P < 0.05$ corrected. Coordinates are reported in RAI order in standard Talairach space.

Post-NFT (compared directly with pre-NFT), the ASD group had significantly higher activation in the right IPL (BA 40). TD participants showed widespread lower activation after NFT, including clusters in bilateral precentral gyrus (BA 4 and 6), right IFG, left IPL and supramarginal gyrus, and bilateral occipital areas. In between-group *t*-tests of post-NFT scans, the significant differences between the ASD and TD groups seen before NFT were absent (i.e., there were no clusters of significant between-group activation differences for the post-NFT scans; Table 4, Fig. 2A and B).

In a whole-brain ANOVA, four significant clusters of interaction between group and training status were observed. These were located in right IPL, left IPL, right precentral gyrus, and left cuneus (Table 5 and Fig. 2C). Follow-up *t*-tests revealed that all of these interactions were driven by post-NFT increases in activation in the ASD group (Cluster in right IPL: pre-NFT β mean = −0.25, SEM = 0.13; post-NFT β mean = 0.71, SEM = 0.23; $P = 0.002$) and by post-NFT decreases in activation in the TD group (pre-NFT β mean = 1.24, SEM = 0.45; post-NFT β mean = −0.20, SEM = 0.24; $P = 0.015$).

Meta-analysis ROI-based analysis

ROI-based ANOVAS performed with activation data within the 14 ROIs based on the meta-analysis (Caspers *et al.*, 2010) showed several main and interaction effects (Table 6, Fig. 3A). There was a main effect of training in the right ventral IPL (referred to as Right SII/IPL by Caspers *et al.*) ($F_{2,15} = 4.76$, $P = 0.037$). There were also significant interaction effects between group and training status in right medial premotor cortex ($F_{2,15} = 6.38$, $P = 0.017$) and right lateral dorsal premotor cortex ($F_{2,15} = 4.48$, $P = 0.0427$). Follow-up *t*-tests suggested that these interactions were driven by inverse trends of slightly increased activations in the ASD group (R med PMC pre-mean β = 0.04, post = 0.36, $P = 0.27$; R lat dPMC pre = −0.27, post = 0.13, $P = 0.27$), vs. slightly decreased activations in the TD group (R med PMC pre-mean β = 0.50, post = −0.45, $P = 0.06$; R lat dPMC; pre = 0.65, post = −0.21, $P = 0.11$).

Imitation task ROI-based analysis

We also observed main and interaction effects within the ROIs based on activation in the present study's imitation task (Table 6, Fig. 3B). There was a main effect of training status in the left postcentral gyrus ROI ($F_{2,15} = 6.62$, $P = 0.015$). There were significant interactions between group and training status in the right IFG ($F_{2,15} = 6.95$, $P = 0.013$) and right precentral gyrus ROIs ($F_{2,15} = 4.5$, $P = 0.042$). Follow-up *t*-tests revealed a similar pattern as the first set of ROIs, with interaction effects reflecting inverse trends of ASD increases (R IFG pre-mean β = 0.45, post = 0.63, $P = 0.64$; R Precentral pre = 0.57, post = 1.00, $P = 0.40$) and TD decreases in activation (R IFG pre-mean β = 1.33, post = −0.003, $P = 0.008$; R Precentral pre = 1.35, post = 0.27, $P = 0.03$).

Covariance of ASD symptom severity and brain activation

In a whole-brain ANCOVA in the ASD group, there was one cluster of significant covariance between post-NFT vs. pre-NFT task activation and changes in the SRS scores. Within this cluster, located in left IPL (Fig. 2D, Table 7), increased activation was correlated with decreased SRS scores (lower symptom severity). In a similar test that used the change in the ATEC scores as a covariate, eight clusters of significant negative correlation were found (Fig. 2D, Table 7), located in left middle/IFG, cerebellum, left superior parietal lobule, right precentral gyrus, left temporal gyrus, left central sulcus, and right cuneus. Like with the SRS scores, increased post-NFT activation was correlated with decreased symptom severity as measured by the ATEC.

Diagnostic symptom severity pre-NFT, as measured by the ADOS-Sociocommunicative subscale, was negatively correlated with increased post- vs. pre-NFT task activation in a cluster in left IPL (Fig. 2D, Table 7). Greater changes in task activation were related to lower initial ASD symptom severity. Scores on the ADI-social subscale did not show significant correlations with activation changes.

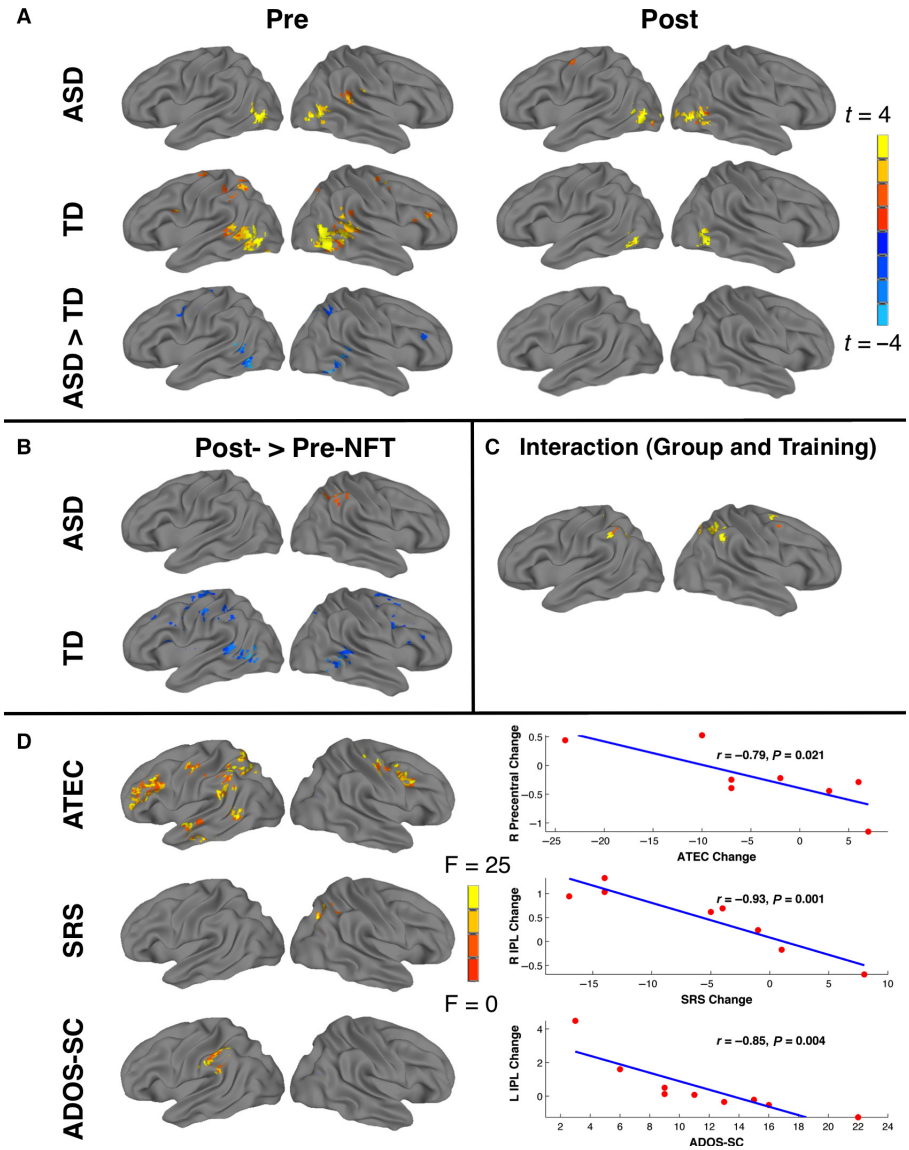

FIG. 2. Task activation results for imitation+observation contrast. (A) Pre- and post-NFT brain activation for ASD, TD ($P < 0.001$ corrected), and group differences (ASD-TD), $P < 0.05$ corrected. (B) Post-NFT minus pre-NFT activation for each group (Top = ASD, Bottom = TD) $P < 0.05$ corrected. (C) ANOVA interaction between group (TD, ASD) and time (pre-NFT, post-NFT), $P < 0.05$ corrected. (D) Significant covariance of NFT-related activation changes with scores on SRS, ATEC, and ADOS Sociocommunicative subscale. $P < 0.05$ corrected. Scatterplots show correlations between changes in activation (Post-Pre NFT) and behavioral/diagnostic scores.

Discussion

The present study investigated the effects of sensorimotor mu-based NFT on imitation-related brain activation. It assessed social behaviors in a group of high-functioning children and adolescents with ASD, compared with a matched group of TD controls. The results show learning during NFT and support the hypothesis that mu-NFT has positive behavioral effects (reduced symptom severity on the ATEC and SRS) in children with ASD. Furthermore, we report for the first time that these benefits are accompanied by – and in fact correlated with – neurophysiological changes in imitation-related brain areas following the training.

Consistent with previous studies (Dapretto *et al.*, 2006), we first predicted that before the NFT, imitation-related brain activation would be atypically reduced in the ASD group in areas associated with imitation and action-observation, including IPL and IFG. In a modified version of an imitation task (Iacoboni, 1999), in which participants imitated and observed object-directed finger movement, TD participants showed significant activation in several areas considered core regions of the hMNS, including IPL, IFG, and STS. In contrast, ASD participants showed a comparatively limited pattern of activation, restricted to visual and posterior temporal areas, during the same task. In a direct comparison between these groups, ASD participants showed significantly lower activation in several areas but most notably in right IFG. As a core area of the hMNS, reduced activation in IFG is indicative of a disruption to this network in the ASD group. This finding, consistent with previous reports (Dapretto *et al.*, 2006), also suggests that increased function in IFG is a potential mechanism for the NFT-related improvements in behavior seen in previous studies.

We predicted that hMNS activation differences between ASD and TD groups would be reduced after NFT, and that this effect would be driven primarily by increases in post-NFT activation in the ASD

TABLE 4. Post-NFT BOLD activation for Imitation + Observation Contrast. All clusters $P < 0.05$ corrected

Group	Peak location	Hemisphere	*x*	*y*	*z*	Voxels	Volume (μL)	Peak *t*-score
TD	Posterior inferior temporal	R	−48	68	−5	35	105	4.02
	Posterior inferior temporal	L	51	64	−5	25	75	3.88
ASD	Posterior inferior/middle temporal	R	−51	68	−5	66	198	3.58
	Posterior inferior/middle temporal	L	51	68	5	47	141	4.77
	Inferior occipital (BA 17)	R	−31	88	−9	22	66	4.25
	Inferior occipital (BA 17)	L	24	88	2	18	54	3.81
	Precentral gyrus (BA 6)	L	44	7	53	16	48	4.40
ASD > TD	No significant clusters	–	–	–	–	–	–	–
ASD only: Post > Pre	Inferior parietal lobule (BA 40)	R	−44	51	46	55	165	2.81
TD only†: Post > Pre	Precentral gyrus (BA 4,6)	L	27	20	66	221	663	−3.14
	Precentral gyrus (BA 6)	R	−34	0	29	86	258	−3.23
	Inferior temporal/lateral occipital	L	51	61	−2	85	255	−3.16
	Cuneus	L	7	71	8	68	204	−3.07
	Middle temporal	R	−61	41	5	67	201	−4.30
	Precuneus	R	−14	75	42	66	198	−2.82
	Supramarginal gyrus (BA 40)	L	31	47	36	54	162	−4.20
	Inferior frontal gyrus (BA 44)	R	−51	−14	15	41	123	−3.60
	Inferior parietal lobule (BA 40)	L	31	44	42	37	111	−2.72
	Precentral gyrus (BA 3)	L	48	20	39	25	75	−2.86

†Subcortical clusters not listed. Coordinates are reported in RAI order in standard Talairach space.

TABLE 5. ANOVA (Group × training status) for Imitation + Observation Contrast. All clusters $P < 0.05$ corrected. No main effects of the group factor were found. Coordinates are reported in RAI order in standard Talairach space

Peak location	Hemisphere	*x*	*y*	*z*	Voxels	Volume (μL)	Peak *F*-score
Main effects: training factor							
Inferior parietal lobule (BA 40)	R	−44	54	42	52	156	14.7
Group × training interactions							
Inferior parietal lobule (BA 40)	R	−44	54	42	224	672	14.7
Inferior parietal lobule (BA 40)	L	37	41	22	79	237	9.46
Precentral gyrus (BA 6)	R	−31	7	49	43	129	15.9
Cuneus (BA 17)	L	20	68	15	40	120	4.34

group. We tested these predictions using two ROI-based approaches. In one, the ROIs were obtained from a meta-analysis (Caspers *et al.*, 2010), while the second approach used activation in the present study's imitation task. Both analyses yielded concordant interaction effects between group and training status in right medial and lateral premotor and inferior frontal regions, driven by activation increases post-NFT in the ASD group, as well as decreases in the TD group. The finding of significant interaction with training in right premotor cortex or right IFG across both sets of ROIs is consistent with our prediction that mu-rhythm NFT would target areas associated with the hMNS. This novel finding supports the idea that neuroplastic changes in these areas are indeed involved in altering the dynamics of mu-rhythm during the NFT process.

We also used a whole-brain field-of-view to test the prediction that NFT would lead to reduced group differences in activation. Using this approach, we found significant interaction effects between group (ASD and TD) and training status (pre-NFT and post-NFT) in four areas: left and right IPL (Brodmann Area 40), right precentral gyrus (BA 6), and left cuneus (BA 17). We also found that the activation changes in right IPL were correlated with our measure of increased volitional control of mu-amplitude across all training sessions, suggesting that the amount of learning that occurs during NFT directly influences the changes occurring in this area of the hMNS. Bilateral IPL is particularly notable because of its role in sensorimotor integration (Andersen, 1987), and in the perception and performance of goal-directed actions (Bonda *et al.*, 1996). Because of these functional associations, and because it is positioned structurally between visual areas and anterior areas of the hMNS (premotor cortex and IFG) (Andersen *et al.*, 1990), IPL is considered a central hMNS hub (Rizzolatti & Craighero, 2004). Therefore, the increased activation in IPL following NFT in the ASD group suggests that this treatment enhanced visuomotor integration between the core areas of the hMNS during imitation in the ASD group.

Interaction effects from both the ROI and whole-brain approaches were driven by the same pattern of group differences in activation. In the regions showing these interaction effects, the TD group showed lower imitation-related activation after NFT, whereas the ASD group showed increased activation. This finding is surprising in view of the behavioral results, which indicated that both groups performed at easy to compare levels on the task both before and after NFT. There were no effects of NFT on overall accuracy for either group, despite the post-NFT changes in activation.

Our final prediction was that the severity of social symptoms in the ASD group would be reduced following training, and that this reduction would correlate with increased hMNS activation during imitation. In the ASD group, there were significant improvements in the SRS and ATEC scores following the NFT. No corresponding changes were seen in the TD group, indicating that the benefits conferred by sensorimotor mu-NFT may specifically benefit children with ASD. The finding of a significant interaction between training status, hMNS activation, and NFT-related changes in the ATEC scores suggests that the behavioral improvements previously observed with NFT (Pineda *et al.*, 2008, 2014) have a neurophysiological basis in hMNS areas. In follow-up *t*-tests, this interaction was driven primarily by increases in hMNS activation, as well as decreases in the ATEC scores (behavioral improvement), in the ASD group following training. Together with the finding of changes in the SRS, this suggests that increases in the hMNS activation resulting from mu-NFT are

TABLE 6. Main effects and interactions for ANOVA between group (ASD and TD) and training status (pre-NFT and post-NFT)

ROI	R/L	Talairach coordinates			Main effect: group		Main effect: training		Interaction	
		x	*y*	*z*	*F*-score	*P*	*F*-score	*P*	*F*-score	*P*
Meta-analysis ROIs (from Caspers *et al.*, 2010)										
Inferior frontal gyrus	L	52	−15	11	0.05	0.82	0.66	0.42	1.08	0.31
Inferior frontal gyrus	R	−52	−19	8	0.22	0.64	0.27	0.60	1.55	0.22
Lat. dorsal premotor	L	31	10	55	0.12	0.73	0.08	0.78	2.76	0.11
Lat. dorsal premotor	R	−38	−7	49	0.98	0.33	0.56	0.46	4.48	0.043*
Med. premotor	L	0	−15	45	0.10	0.75	0.27	0.61	1.54	0.22
Med. premotor	R	−13	−9	57	0.50	0.49	1.59	0.22	6.38	0.017*
Intraparietal sulcus	L	33	35	46	2.22	0.15	3.54	0.07	3.19	0.08
Inferior parietal lobule	R	−47	32	47	4.04	0.05	4.28	0.047	1.89	0.18
Sup. temporal sulcus	L	47	45	11	1.04	0.32	0.01	0.91	1.05	0.31
Inferior parietal lob. 2	R	−54	22	18	0.02	0.88	4.76	0.037*	0.07	0.80
Lat. occipital	L	45	65	8	0.01	0.94	0.01	0.91	0.68	0.41
Lat. occipital	R	−48	59	6	0.25	0.62	0.58	0.45	1.98	0.17
Anterior insula	R	−38	−7	0	0.68	0.41	1.96	0.17	0.8	0.38
Fusiform face area	R	−40	49	−17	3.34	0.08	0.01	0.9112	2.31	0.14
Seeds derived from imitation task										
Post. mid. temporal	L	−49	54	4	2.55	0.12	3.13	0.087	2.48	0.12
Post. mid. temporal	R	47	57	4	0.66	0.42	2.42	0.13	1.4	0.25
Superior parietal lob.	L	27	52	47	1.03	0.32	3.13	0.087	3.67	0.06
Inferior parietal lob.	R	−33	46	47	0.02	0.89	0.43	0.52	1.39	0.25
Postcentral gyrus	L	52	22	28	0.55	0.47	6.62	0.015*	3.08	0.09
Precentral gyrus	R	−40	9	47	0	0.95	0.83	0.37	4.5	0.042*
Inferior frontal gyrus	R	−46	−16	16	0.17	0.68	4.09	0.052	6.95	0.013*

*Significant main effects or interactions.

accompanied by positive changes in personal behavior as measured by parental assessment.

In addition to using tests designed to measure longitudinal changes in behavior, we also investigated the relationship between initial severity of ASD symptoms and NFT-related neurophysiological outcomes. The results indicated a link between the magnitude of changes in activation in left IPL (before vs. after NFT) and pre-training ADOS scores. Specifically, greater NFT-related changes were negatively correlated with ADOS scores. This suggests that the particular regimen of NFT used in this study is most beneficial to individuals on the highest end of the functional autism spectrum. The correlation between hours of training completed and ADOS scores (social and communicative subscales combined) was not significant, suggesting that this effect of initial symptom severity on NFT-induced activation changes was not the result of participants with more severe symptoms completing fewer hours of training ($r = 0.02$, $P = 0.96$). Taken together, these neurophysiological and behavioral findings indicate that the NFT can improve the functionality of the hMNS, resulting in greater recruitment of previously underutilized areas, and that these neurofunctional changes are linked to improvements in core ASD symptomatology.

While the results of the present study are novel and potentially highly significant, there are some caveats to their interpretation. One limitation was the lack of a sham treatment condition, in which the feedback received by participants during training sessions would not reflect their live EEG signal but instead might be based on the signal from a previously recorded session. Parents were aware that their children received an active treatment, and an expectation of behavioral improvements may have affected their ratings on SRS and ATEC questionnaires. However, the correlations between caretaker assessments and changes in brain activation suggest that the behavioral changes did in fact have an underlying neurophysiological basis in areas related to action-observation and imitation. Furthermore, the comparison to a TD group helped control for nonspecific factors accounting for the efficacy of mu-NFT. A frequent criticism of studies of the clinical efficacy of NFT is that a number of psychosocial and expectancy effects could be a larger factor in the results than the NFT itself (Thibault *et al.*, 2016). In the present study, the lack of similar changes in both groups suggests that our protocol not only had an effect on the areas we predicted, but did so specifically for ASD participants.

It is also worth noting that while our NFT protocol specifically rewarded increasing amplitude in the mu-frequency band, this was accompanied by a requirement that participants minimize amplitude in the theta and beta bands. Some previous studies have shown improvements in executive function in children with ASD after NFT specifically targeting the theta and beta bands (Kouijzer *et al.*, 2009). While the hypotheses of the present study drew largely from the evidence often used to support the so-called 'broken mirror' hypothesis of ASD (Williams *et al.*, 2001; Ramachandran & Oberman, 2006; Fox *et al.*, 2016), we make the important distinction that hMNS dysfunction in ASD appears to be context-dependent (McIntosh *et al.*, 2006; Oberman *et al.*, 2008), and therefore, potentially improvable. In this way, any side-effects of theta and beta regulation on brain regions involved in attention and executive function may have had a synergistic effect on the results we found in the hMNS areas. However, it was beyond the scope of the present study to determine the contribution of such secondary factors to the effects of mu-NFT. Therefore, although the EEG signal rewarded in our NFT protocol was recorded over an area of sensorimotor cortex known to generate the functionally distinct mu-rhythm (Manshanden *et al.*, 2002), we cannot completely rule out the contribution of theta and beta regulation, and the possible role of changes in executive function, to the post-NFT effects we have observed.

This study also lacked a control task designed to test the effects of mu-NFT on a nonsocial cognitive ability such as working memory. We prioritized minimal scan length and reduced task complexity, in light of the already stressful nature of undergoing an fMRI scan for children, particularly those with ASD. A lack of post-NFT

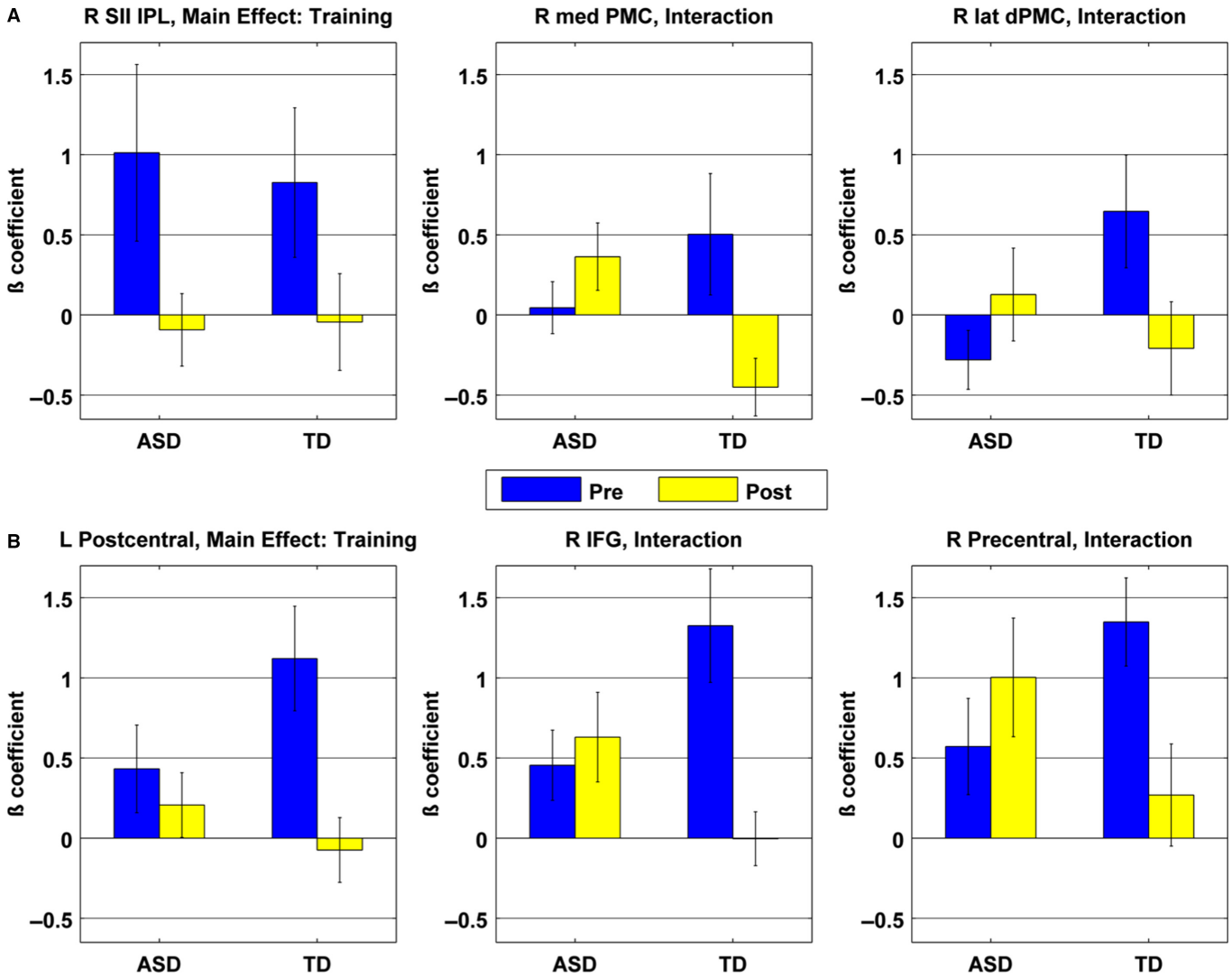

FIG. 3. (A) Significant main effects and interactions for imitation + observation contrast activation within regions of interest based on a meta-analysis of imitation (Caspers *et al.*, 2010). (B) Significant main effects and interactions for activation within regions of interest based on areas of significant activation during the imitation + observation contrast.

TABLE 7. Areas of activation showing significant covariance with diagnostic assessment scores (ASD only). Cluster corrected to $P < 0.05$. Coordinates for each cluster's center of mass are in standard Talairach space

Group	Peak location	Hemi	*x*	*y*	*z*	Voxels	Volume (μL)	Mean covar.	Mean *Z*-score
SRS	SPL/Precuneus	R	−27	58	32	50	150	−0.11	−3.73
ATEC	IFG/MFG (BA 9,46)	L	48	−17	29	120	360	−0.10	−4.10
	Post. MTG	L	41	58	2	66	198	−0.09	−4.65
	Cuneus	R/L	0	75	22	66	198	−0.11	−4.23
	Cerebellum	L	3	75	−33	62	186	−0.24	−4.72
	MTG/STG (BA 21,22)	L	44	13	−16	56	168	−0.15	−4.61
	IPL	L	58	44	25	49	147	−0.10	−4.13
	Precentral gyrus	R	−41	3	49	49	147	−0.07	−4.29
	SPL	L	20	64	56	46	138	−0.23	−4.28
ADOS-SC	Inferior parietal lobule (BA 40)	L	54	27	36	71	213	−0.35	−3.79

effects on such a task may have helped demonstrate that the neurophysiological effects of mu-NFT are specific to areas involved in the imitation of biological motion. However, as we used a whole-brain field-of-view to test for brain activation, and found post-NFT interaction effects in areas associated with the hMNS, we are confident in the specificity of mu-NFT effects on this system. An additional limitation is the relatively small final sample size, due in part to attrition associated with the time-consuming nature of NFT across many sessions and weeks, and to excessive head motion in some participants. However, detection of significant group and post-training effects even in this relatively small sample suggests that mu-NFT effects are robust.

Our findings suggest that in children and adolescents with ASD, sensorimotor mu-NFT has significant positive effects on social behaviors, as well as on the neurofunctional substrates of those behaviors, potentially centered on mirror neuron networks. While similar NFT protocols have previously been shown to positively influence electrophysiological signatures of mirror neuron networks in autism, this is the first study using fMRI to directly localize effects of mu-NFT on brain regions involved in action-observation and imitation. The finding of strong correlations between behavioral improvements and activation changes specifically in these brain regions supports the use of mu-NFT to improve clinical outcomes for individuals on the autism spectrum.

Supporting Information

Additional supporting information can be found in the online version of this article:

Data S1. Supplementary methods.

Fig. S1. Correlations between pre-NFT diagnostic assessment scores (ADOS-SC, ADI-SOC, and ADI-COM) and changes in parental assessments of behavior following NFT (ATEC, SRS).

Table S1. Pearson correlations for clinical assessment scores vs. post-pre-NFT changes in parental assessment scores.

Table S2. Pre-NFT BOLD activation for Imitation Contrast. All clusters $P < 0.05$ corrected.

Table S3. Pre-NFT BOLD activation for Observation Contrast. All clusters $P < 0.05$ corrected.

Table S4. Post-NFT BOLD activation for Imitation Contrast. All clusters $P < 0.05$ corrected.

Table S5. Post-NFT BOLD activation for Observation Contrast. All clusters $P < 0.05$ corrected.

Table S6. ANOVA (Group × Training status) for Imitation Contrast.

Table S7. Main effects and interactions for ANOVA between group (ASD and TD) and training status (pre-NFT and post-NFT) for Imitation contrast.

Table S8. Main effects and interactions for ANOVA between group (ASD and TD) and training status (pre-NFT and post-NFT) for Observation contrast.

Acknowledgments

The authors would like to thank Dr. Lisa Eyler, Dr. Terry Jernigan, and Dr. Ayşe Saygin for technical and theoretical advice. We would also like to thank Summer Moss for her assistance with data collection. We thank the Congressionally Directed Medical Research Programs for an Autism Research Program (ARP) Idea Award (CDMRP-AR093335) to J.P.

Conflict of interest

All authors declare that they have no conflicts of interest.

Author contributions

MD designed fMRI experiment, collected and analyzed data, drafted paper. JP designed neurofeedback protocol, worked on paper. RM provided fMRI support and worked on paper.

Data accessibility

Due to data size and participant privacy issues, code for task presentation, data preprocessing, and analysis, as well as the raw data itself is not publically archived. Please contact the corresponding author if you wish to obtain any of these materials.

Abbreviations

ADI, Autism Diagnostic Interview; ADOS, Autism Diagnostic Observation Schedule; ANCOVA, analysis of covariance; ANOVA, analysis of variance; ASD, autism spectrum disorder; ATEC, Autism Treatment Evaluation Checklist; EEG, electroencephalography; fMRI, functional magnetic resonance imaging; hMNS, human mirror neuron system; IFG, inferior frontal gyrus; IPL, inferior parietal lobule; NFT, neurofeedback training; SRS, Social Responsiveness Scale; STS, superior temporal sulcus; TD, typically developing; WASI, Wechsler Abbreviated Scale of Intelligence.

References

Andersen, R.A. (1987) Inferior parietal lobule function in spatial perception and visuomotor integration. In Plum, F., Mountcastle, V.B. & Geiger, S.R. (Eds), *Handbook of Physiology. Section 1: The Nervous System vol. V, Part 2. Higher Functions of the Brain*,. American Physiological Society, Bethesda, MD, pp. 483–518.

Andersen, R.A., Asanuma, C., Essick, G. & Siegel, R.M. (1990) Corticocortical connections of anatomically and physiologically defined subdivisions within the inferior parietal lobule. *J. Comp. Neurol.*, **296**, 65–113.

Arnstein, D., Cui, F., Keysers, C., Maurits, N.M. & Gazzola, V. (2011) μ-Suppression during action observation and execution correlates with BOLD in dorsal premotor, inferior parietal, and SI cortices. *J. Neurosci.*, **31**, 14243–14249.

Baron-Cohen, S. (2009) Autism: the empathizing-systemizing (E-S) theory. *Ann. NY Acad. Sci.*, **1156**, 68–80.

Bernier, R., Dawson, G., Webb, S. & Murias, M. (2007) EEG mu rhythm and imitation impairments in individuals with autism spectrum disorder. *Brain Cognition*, **64**, 228–237.

Bonda, E., Petrides, M., Ostry, D. & Evans, A. (1996) Specific involvement of human parietal systems and the amygdala in the perception of biological motion. *J. Neurosci.*, **16**, 3737–3744.

Braadbaart, L., Williams, J.H. & Waiter, G.D. (2013) Do mirror neuron areas mediate mu rhythm suppression during imitation and action observation? *Int. J. Psychophysiol.*, **89**, 99–105.

Buccino, G., Binkofski, F., Fink, G.R., Fadiga, L., Fogassi, L., Gallese, V., Seitz, R.J., Zilles, K. *et al.* (2001) Action observation activates premotor and parietal areas in a somatotopic manner: an fMRI study. *Eur. J. Neurosci.*, **13**, 400–404.

Cahan, S. & Noyman, A. (2001) The Kaufman ability battery for children mental processing scale: a valid measure of "pure" intelligence? *Educ. Psychol. Meas.*, **61**, 827–840.

Carpenter, M., Nagell, K. & Tomasello, M. (1998) Social cognition, joint attention, and communicative competence from 9 to 15 months of age. *Monogr. Soc. Res. Child*, **63**, i-174.

Caspers, S., Zilles, K., Laird, A.R. & Eickhoff, S.B. (2010) ALE meta-analysis of action observation and imitation in the human brain. *NeuroImage*, **50**, 1148–1167.

Coben, R., Linden, M. & Myers, T.E. (2010) Neurofeedback for autistic spectrum disorder: a review of the literature. *Appl. Psychophys. Biof.*, **35**, 83–105.

Coben, R., Sherlin, L., Hudspeth, W.J., McKeon, K. & Ricca, R. (2014) Connectivity-guided EEG biofeedback for autism spectrum disorder: evidence of neurophysiological changes. *NeuroRegulation*, **1**, 109.

Constantino, J.N., Davis, S.A., Todd, R.D., Schindler, M.K., Gross, M.M., Brophy, S.L., Metzger, L.M., Shoushtari, C.S. *et al.* (2003) Validation of a brief quantitative measure of autistic traits: comparison of the social responsiveness scale with the autism diagnostic interview-revised. *J. Autism Dev. Disord.*, **33**, 427–433.

Dapretto, M., Davies, M.S., Pfeifer, J.H., Scott, A.A., Sigman, M., Bookheimer, S.Y. & Iacoboni, M. (2006) Understanding emotions in others: mirror neuron dysfunction in children with autism spectrum disorders. *Nat. Neurosci.*, **9**, 28–30.

Dinstein, I., Thomas, C., Behrmann, M. & Heeger, D.J. (2008) A mirror up to nature. *Curr. Biol.*, **18**, 13–18.

DiPelligrino, G., Fadiga, L., Fogassi, L., Gallese, V. & Rizzolatti, G. (1992) Understanding motor events: a neurophysiological study. *Exp. Brain Res.*, **91**, 176–180.

Fishman, I., Datko, M., Cabrera, Y., Carper, R.A. & Müller, R.A. (2015) Reduced integration and differentiation of the imitation network in autism: a combined functional connectivity magnetic resonance imaging and diffusion-weighted imaging study. *Ann. Neurol.*, **78**, 958–969.

Forman, S.D., Cohen, J.D., Fitzgerald, M., Eddy, W.F., Mintun, M.A. & Noll, D.C. (1995) Improved assessment of significant activation in functional magnetic resonance imaging (fMRI): use of a cluster-size threshold. *Magn. Reson. Med.*, **33**, 636–647.

Fox, D.J., Tharp, D.F. & Fox, L.C. (2005) Neurofeedback: an alternative and efficacious treatment for Attention Deficit Hyperactivity Disorder. *Appl. Psychophys. Biof.*, **30**, 365–373.

Fox, N.A., Bakermans-Kranenburg, M.J., Yoo, K.H., Bowman, L.C., Cannon, E.N., Vanderwert, R.E., Ferrari, P.F. & van IJzendoorn, M.H. (2016) Assessing human mirror activity with EEG Mu rhythm: a meta-analysis. *Psychol. Bull.*, **142**, 291–313.

Fuchs, T., Birbaumer, N., Lutzenberger, W., Gruzelier, J.H. & Kaiser, J. (2003) Neurofeedback treatment for attention-deficit/hyperactivity disorder in children: a comparison with methylphenidate. *Appl. Psychophys. Biof.*, **28**, 1–12.

Hadjikhani, N., Joseph, R.M., Snyder, J. & Tager-Flusberg, H. (2006) Anatomical differences in the mirror neuron system and social cognition network in autism. *Cereb. Cortex*, **16**, 1276–1282.

Hamilton, A.F.D.C. (2013) Reflecting on the mirror neuron system in autism: a systematic review of current theories. *Dev. Cogn. Neurosci.*, **3**, 91–105.

Hari, R., Forss, N., Avikainen, S., Kirveskari, E., Salenius, S. & Rizzolatti, G. (1998) Activation of human primary motor cortex during action observation: a neuromagnetic study. *Proc. Natl. Acad. Sci. USA*, **95**, 15061–15065.

Hickok, G. (2009) Eight problems for the mirror neuron theory of action understanding in monkeys and humans. *J. Cogn. Neurosci.*, **21**, 1229–1243.

Iacoboni, M. (1999) Cortical mechanisms of human imitation. *Science*, **286**, 2526–2528.

Kouijzer, M.E., de Moor, J.M., Gerrits, B.J., Congedo, M. & van Schie, H.T. (2009) Neurofeedback improves executive functioning in children with autism spectrum disorders. *Res. Autism Spect. Dis.*, **3**, 145–162.

Lévesque, J., Beauregard, M. & Mensour, B. (2006) Effect of neurofeedback training on the neural substrates of selective attention in children with attention-deficit/hyperactivity disorder: a functional magnetic resonance imaging study. *Neurosci. Lett.*, **394**, 216–221.

Lord, C., Risi, S., Lambrecht, L., Cook, E.H., Leventhal, B.L., DiLavore, P.C., Pickles, A. & Rutter, M. (2000) The Autism Diagnostic Observation Schedule—Generic: a standard measure of social and communication deficits associated with the spectrum of autism. *J. Autism Dev. Disord.*, **30**, 205–223.

Magiati, I., Moss, J., Yates, R., Charman, T. & Howlin, P. (2011) Is the Autism Treatment Evaluation Checklist a useful tool for monitoring progress in children with autism spectrum disorders? *J. Intell. Disabil. Res.*, **55**, 302–312.

Manshanden, I., De Munck, J.C., Simon, N.R. & da Silva, F.H.L. (2002) Source localization of MEG sleep spindles and the relation to sources of alpha band rhythms. *Clin. Neurophysiol.*, **113**, 1937–1947.

Martineau, J., Cochin, S., Magne, R. & Barthelemy, C. (2008) Impaired cortical activation in autistic children: is the mirror neuron system involved? *Int. J. Psychophysiol.*, **68**, 35–40.

Martineau, J., Andersson, F., Barthélémy, C., Cottier, J.P. & Destrieux, C. (2010) Atypical activation of the mirror neuron system during perception of hand motion in autism. *Brain Res.*, **1320**, 168–175.

McFarland, D.J., Miner, L.A., Vaughan, T.M. & Wolpaw, J.R. (2000) Mu and beta rhythm topographies during motor imagery and actual movements. *Brain Topogr.*, **12**, 177–186.

McIntosh, D.N., Reichmann-Decker, A., Winkielman, P. & Wilbarger, J.L. (2006) When the social mirror breaks: deficits in automatic, but not voluntary, mimicry of emotional facial expressions in autism. *Developmental Sci.*, **9**, 295–302.

Misra, V. (2014) The social brain network and autism. *Ann. Neurol.*, **21**, 69–73.

Muthukumaraswamy, S.D., Johnson, B.W. & McNair, N.A. (2004) Mu rhythm modulation during observation of an object-directed grasp. *Brain Res. Cogn. Brain Res.*, **19**, 195–201.

Nishitani, N., Avikainen, S. & Hari, R. (2004) Abnormal imitation-related cortical activation sequences in Asperger's syndrome. *Ann. Neurol.*, **55**, 558–562.

Oberman, L.M. & Ramachandran, V.S. (2007) The simulating social mind: the role of the mirror neuron system and simulation in the social and communicative deficits of autism spectrum disorders. *Psychol. Bull.*, **133**, 310–327.

Oberman, L.M., Hubbard, E.M., McCleery, J.P., Altschuler, E.L., Ramachandran, V.S. & Pineda, J.A. (2005) EEG evidence for mirror neuron dysfunction in autism spectrum disorders. *Brain Res. Cogn. Brain Res.*, **24**, 190–198.

Oberman, L.M., Ramachandran, V.S. & Pineda, J.A. (2008) Modulation of mu suppression in children with autism spectrum disorders in response to familiar or unfamiliar stimuli: the mirror neuron hypothesis. *Neuropsychologia*, **46**, 1558–1565.

Oberman, L.M., McCleery, J.P., Hubbard, E.M., Bernier, R., Wiersema, J.R., Raymaekers, R. & Pineda, J.A. (2013) Developmental changes in mu suppression to observed and executed actions in autism spectrum disorders. *Soc. Cogn. Affect. Neur.*, **8**, 300–304.

Othmer, S. (2012). *Protocol Guide for Neurofeedback Clinicians*. EEG Info, Woodland Hills, CA.

Pelphrey, K.A. & Carter, E.J. (2008) Brain mechanisms for social perception. *Ann. N. Y. Acad. Sci.*, **1145**, 283–299.

Perkins, T., Stokes, M., McGillivray, J. & Bittar, R. (2010) Mirror neuron dysfunction in autism spectrum disorders. *J. Clin. Neurosci.*, **17**, 1239–1243.

Pfurtscheller, G. & Neuper, C. (1994) Event-related synchronization of mu rhythm in the EEG over the cortical hand area in man. *Neurosci. Lett.*, **174**, 93–96.

Pfurtscheller, G., Neuper, C. & Krausz, G. (2000) Functional dissociation of lower and upper frequency mu rhythms in relation to voluntary limb movement. *Clin. Neurophysiol.*, **111**, 1873–1879.

Pfurtscheller, G., Brunner, C., Schlögl, A. & Lopes da Silva, F.H. (2006) Mu rhythm (de)synchronization and EEG single-trial classification of different motor imagery tasks. *NeuroImage*, **31**, 153–159.

Pineda, J.A. (2005) The functional significance of mu rhythms: translating "seeing" and "hearing" into "doing". *Brain Res. Brain Res. Rev.*, **50**, 57–68.

Pineda, J.A. (2009). Mirror neuron systems. *The Role of Mirroring Processes in Social Cognition*. Humana Press, New York.

Pineda, J.A., Allison, B.Z. & Vankov, A. (2000) Self-movement, observation, and imagination effects on Mu rhythm and readiness potentials (RPs): towards a brain-computer interface (BCI). *IEEE T. Rehabil. Eng.*, **8**, 219–222.

Pineda, J.A., Brang, D., Hecht, E., Edwards, L., Carey, S., Bacon, M., Futagaki, C., Suk, D. *et al.* (2008) Positive behavioral and electrophysiological changes following neurofeedback training in children with autism. *Res. Autism Spect. Dis.*, **2**, 557–581.

Pineda, J.A., Juavinett, A. & Datko, M. (2012) Self-regulation of brain oscillations as a treatment for aberrant brain connections in children with autism. *Med. Hypotheses*, **79**, 790–798.

Pineda, J.A., Carrasco, K., Datko, M., Pillen, S. & Schalles, M. (2014) Neurofeedback training produces normalization in behavioural and electrophysiological measures of high-functioning autism. *Philos. T. Roy. Soc. B*, **369**, 20130183.

Ramachandran, V.S. & Oberman, L.M. (2006) Broken mirrors: a theory of autism. *Sci. Am.*, **295**, 62–69.

Rizzolatti, G. & Craighero, L. (2004) The mirror-neuron system. *Annu. Rev. Neurosci.*, **27**, 169–192.

Ros, T., Munneke, M.A.M., Ruge, D., Gruzelier, J.H. & Rothwell, J.C. (2010) Endogenous control of waking brain rhythms induces neuroplasticity in humans. *Eur. J. Neuorsci.*, **31**, 770–778.

Roth, S.R., Sterman, M.B. & Clemente, C.D. (1967) Comparison of EEG correlates of reinforcement, internal inhibition, and sleep. *Electroen. Clin. Neuro.*, **23**, 509–520.

Rutter, M., Le Couteur, A. & Lord, C. (2003) *Autism Diagnostic Interview-Revised*, Vol. **29**. Western Psychological Services, Los Angeles, CA, 30.

Sterman, M.B. (1996) Physiological origins and functional correlates of EEG rhythmic activities: implications for self-regulation. *Biofeedback Self-Reg.*, **21**, 3–33.

Talairach, J. & Tournoux, P. (1988) Co-planar stereotaxic atlas of the human brain. 3-Dimensional proportional system: an approach to cerebral imaging. Thieme Medical Publishers, New York.

Théoret, H., Halligan, E., Kobayashi, M., Fregni, F., Tager-Flusberg, H. & Pascual-Leone, A. (2005) Impaired motor facilitation during action observation in individuals with autism spectrum disorder. *Curr. Biol.*, **15**, R84–R85.

Thibault, R.T., Lifshitz, M. & Raz, A. (2016) The self-regulating brain and neurofeedback: experimental science and clinical promise. *Cortex*, **74**, 247–261.

Turella, L., Pierno, A.C., Tubaldi, F. & Castiello, U. (2009) Mirror neurons in humans: consisting or confounding evidence? *Brain Lang.*, **108**, 10–21.

Walker, J.E. (2008) Power spectral frequency and coherence abnormalities in patients with intractable epilepsy and their usefulness in long-term remediation of seizures using neurofeedback. *Clin. EEG Neurosci.*, **39**, 203–205.
Wechsler, D. (1999). *Wechsler Abbreviated Scale of Intelligence*. Psychological Corporation, San Antonio, Texas.
Williams, J.H., Whiten, A., Suddendorf, T. & Perrett, D.I. (2001) Imitation, mirror neurons and autism. *Neurosci. Biobehav. R.*, **25**, 287–295.
Williams, J.H.G., Waiter, G.D., Gilchrist, A., Perrett, D.I., Murray, A.D. & Whiten, A. (2006) Neural mechanisms of imitation and "mirror neuron" functioning in autistic spectrum disorder. *Neuropsychologia*, **44**, 610–621.